16TH EUROPEAN CONFERENCE ON EARTHQUAKE ENGINEERING THESSALONIKI 18 - 21 JUNE 2018

A STUDY ON THE SEISMIC VULNERABILITY OF A SELECTED PETROCHEMICAL PLANT PIPING SYSTEM

Stefano CAPRINOZZI[1], Jure ŽIŽMOND[2], Fabrizio PAOLACCI[3], Matjaž DOLŠEK[4]

ABSTRACT

In order to better understand vulnerability of existing components of petrochemical plants, it is necessary to develop computationally efficient and still accurate procedures for the evaluation of the fragility curves of such components. However, petrochemical plants can be extremely complex systems, which means that computational efficiency becomes very challenging issue. Thus researchers investigated how to reduce the number of simulations, which are necessary to calculate fragility curves. In this paper the so-called 3R (Record selection, Response analysis, Risk-based decision making) method was used in order to demonstrate its computational efficiency and accuracy. The method requires assessment of seismic performance at only one level of design seismic action and enables decision whether the fragility curve is on the left or the right hand side of the target fragility curve, which is calculated on the basis of the target risk, known hazard function and assumed dispersion of the limit-state seismic intensity of the investigated component. In the first part of the paper, the theoretical background of the 3R method is summarized and then demonstrated by means of an example of petrochemical plant located in Sicily. The results of the investigation are compared with the results obtained by incremental dynamic analysis (IDA) and multiple stripes analysis (MSA). Different intensity measures have been used aimed at investigating the impact of intensity measure on the estimated risk of exceedance limit states of pipes and structure. Results of fragility analyses have showed greater vulnerability of pipes with respect of the structural collapse. It is also shown that 3R method provided correct risk-based decision making even in the case when the target risk was very close to the estimated risk.

Keywords: Petrochemical Plants; Fragility Analysis; 3R Method; Risk; Nonlinear Time-History Analysis; Target Risk.

1. INTRODUCTION

Industrial hazardous facilities are nowadays extremely important for the functionality of built environment and community. Moreover, the increased environmental attention and the fear of economic losses, new tools, which are capable to prior quantify and assess risks and losses, are required more than ever. Recent events displayed lacks of adequacy against seismic actions and several failures and significant damages on support structures, piping systems and their components were observed after major earthquakes, as reported in several publications as (Paolacci et al., 2013). In order to adequately quantify risk and resilience of such complex infrastructural systems, numerous analyses of non-linear models and sophisticated approaches are needed. However, such tasks are extremely demanding in terms of computational time. On the other hand, there are no satisfactory codes and standards, which would prescribe the use of probabilistic methods for design or seismic performance assessment of such systems. The adequacy of fragility curves was checked for a typical refinery piping system using 3R method (Dolšek & Brozovič, 2016), while fragility curves were estimated by using incremental dynamic analysis (IDA) (Vamvatsikos & Cornell, 2002) and multiple stripes analysis (MSA) (Jalayer, 2003). Fragility functions were estimated for peak ground acceleration and spectral acceleration at fundamental vibration mode. Finally, results are presented, compared and discussed.

[1]PhD. Student, University of Ljubljana, Ljubljana, Slovenia, stefano.caprinozzi@fgg.uni-lj.si
[2]Assistant. Department, University of Ljubljana, Ljubljana, Slovenia, jure.zizmond@fgg.uni-lj.si
[3]Prof., Department, University of Roma Tre, Rome, Italy, fabrizio.paolacci@uniroma3.it
[4]Prof., Department, University of Ljubljana, Ljubljana, Slovenia, matjaz.dolsek@fgg.uni-lj.si

2. UNIVARIATE FRAGILITY MODEL

Structural fragility can be defined as the probability of exceeding a designated limit state (*LS*) (e.g. collapse) for a given value of intensity measure (*IM*). The *LS* is usually defined by means of a threshold value of Engineering Demand Parameters (*EDPs*). In this study, the strain in the structural elements and the stress on pipes were selected as the *EDPs*. The limit-state values of the strain and the stress were estimated by IDA and MSA. Single Stipe Analysis (SSA) was also used in the context of 3R method. The fragility models associated with response of structures are often defined as univariate since only one quantity is to be predicted. Multivariate fragility models were recently used and developed by means of different variables, for instance *IM* and damage level (*D*) as (Zentner, 2017), but in this paper, *D* has been treated as deterministic. The conditional probability (*P*) is usually given by the lognormal Cumulative Distribution Function (*CDF*) of ground motions (*GMs*) intensity. The objective is to estimate the quantities needed for the fragility functions defined in Equation 1:

$$\text{Fragility function} = P\left(D_{EDP} > LS \mid IM = x \right) = \Phi\left(\frac{\ln \frac{x}{\theta}}{\beta} \right) \tag{1}$$

where *LS* is the limit state of interest, *IM* is the ground-motion intensity measure, usually peak ground acceleration (*PGA*) or spectral acceleration at fundamental vibration period *T*, $S_a(T)$, *x* is the value of the ground-motion intensity measure, Φ (·) is the cumulative distribution function of standardized normal distribution, θ is the mean of *IM* causing *LS* and β is the corresponding standard deviation of logarithmic values. A sample of *IMs* causing *LS* can be calculated with different methods of analysis, e.g. by IDA and MSA. The results are then post-processed in order to obtain median and dispersion with the maximum likelihood method in Equation 2 and 3 for IDA and MSA respectively. Equation 3 represents the logarithm form of the maximum likelihood because it is mathematically equivalent and easier to maximize the logarithm of the likelihood instead the classical function, (Baker, 2014). It has been computed by using Matlab (MathWorks, 2012):

$$\ln\theta = \frac{1}{n}\sum_{i=1}^{n} \ln IM_i \qquad \beta = \sqrt{\frac{1}{n-1}\sum_{i=1}^{n}\left(\ln \frac{IM_i}{\theta} \right)^2} \tag{2}$$

$$\{\theta, \beta\} = \arg\max_{\theta,\beta} \sum_{i=1}^{m} \left\{ \ln \binom{n_j}{z_j} + zj \ln \Phi\left(\frac{\ln \frac{x_j}{\theta}}{\beta} \right) + \left(n_j - z_j \right) \ln\left(1 - \Phi\left(\frac{\ln \frac{x_j}{\theta}}{\beta} \right) \right) \right\} \tag{3}$$

where *n* represents the number of ground motions considered, IM_i is the intensity of the *i-th* ground motion exceeding *LS*, *m* represents the number of steps for *IM*, n_j the number of ground motions at intensity *j*, z_j the number of ground motions exceeding *LS* at intensity *j* and x_j is the intensity measure value.

3. DESCRIPTION OF CASE STUDY

The selected case study, Figure 1, is a part of a petrochemical plant located in Sicily, a high seismicity region in Southern Italy. It contains 8" (inches) straight pipes, several elbows and weld-neck bolted flange joints (*BFJs*). Pipes are made of API 5L Gr.X52 steel (nominal yield strengths 418 MPa and ultimate strengths 554 MPa) filled with liquid at an internal pressure of 5 MPa. The support structure is a steel frame structure, with six bays of six meters span each, 12 and 10.5 m high, mainly composed of S275 steel HE profiles and some vertical and horizontal bracings, (Caprinozzi et al., 2017).

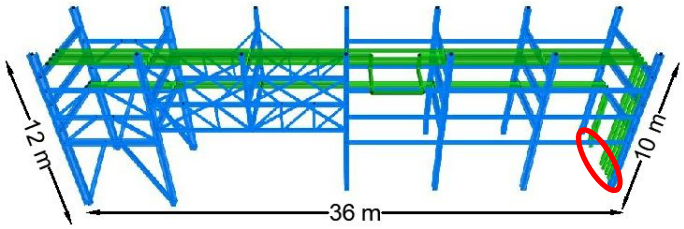

Figure 1. View of the case study and pipes fully restrained to ground (CSI, 2011).

4. NUMERICAL MODELLING

In order to evaluate the seismic response of the structure and the pipes, a finite element model was developed in OpenSees (McKenna & Fenves, 2010) neglecting specific modelling of elbows and *BFJs*. The presence of internal liquid contained by pipes were considered by increasing the mass property of the material. In addition, the internal pressure was neglected as well. In this respect fiber discretized beam element models were adopted for structure and pipes both and Menegotto-Pinto model was used as the constitutive law of steel, assigned to each fiber. E_s=205/210 GPa f_y=275/418 MPa for support structure and pipes, respectively. Boundary conditions of pipes are extremely important because they seriously affect the seismic behavior of the structure (Bursi et al 2016). In this respect all the pipes have been assumed fully restrained to the steel support structure, by means of rigid links, and their ends were supposed fully restrained to the ground to one side of the structure only, simulating the presence of external structure or pipes, and free to move according to the structure displacements to the other side.

4.1 Interaction Between Pipes and Support Structure

Many authors spent several time investigating the influence of pipes to the beneath structure as (Aparna & Vinay k., 1998), (Azizpour & Hosseisni, 2009), but the evidences of the dynamic coupling interaction are not so easy to be obtained and, more in general a common rule cannot be established because the dynamic behavior depends simultaneously on different factors. However, some codes trying to address the problem providing rules. More in detail ASCE (Task Committee on Seismic Evaluation and Design of Petrochemical Facilities of ASCE, 2011) foresees that if the ratio between the weights of pipes and supporting structure (*WR*) is less than 0,25 the dynamic interaction between the pipes and the structure can be neglected. Even though this aspect would deserve more attention (Bursi et al 2015), in the present example the simple *ASCE* rule has been adopted. Accordingly, because *WR* > 0,25 the dynamic interaction cannot be neglected and it must be taken into account by modelling pipes and structure in the same model. In fact, comparing the vibration periods of two models, i.e. with and without pipes, it was observed that the presence of pipes is indeed important for the seismic analysis (Paolacci et al 2011).

5. SEISMIC VULNERABILITY ASSESSMENT

5.1 Ground Motion Selection

The most common target spectrum for ground-motion selection is the uniform hazard spectrum (*UHS*) but it has been found unsuitable as it conservatively implies that large-amplitude spectral values will occur at all periods within a single ground motion (Baker, 2010). Hence in this paper the conditional mean spectrum (*CMS*) is used. The spectral acceleration (S_a) at the fundamental vibration period (T=0.28 s) and *PGA* were assumed as the seismic *IM* for the selection of *GMs*. Ground motions were selected according to the algorithm proposed by (Jayaram et al., 2011). All sets of *GMs* were selected from the Strong ground motion database which contains 9188 ground motions from the *NGA* (Chiou et al., 2008) and the *RESORCE* (Akkar et al., 2014) database. The two databases were recently combined by The Institute of Structural Engineering, Earthquake Engineering and Construction IT (*IKPIR*) by (Šebenik & Dolšek, 2016). The selected *GMs* correspond to events within 5-50 km and magnitudes range 4.5 - 7.

Table 1 presents all sets of *GMs* adopted. For IDA, ground motions sets #1 and #2 have been selected based conditional target spectra (*CS*) and it was defined by using the results of *SHARE* project (Woessner et al., 2015). The *CS* was defined based on the results of the seismic hazard disaggregation for the site and by adopting the mean return period of 2475 years in the case of *PGA* and $S_a(0.28)$, i.e. the vibration period with the highest modal mass. 3R Method has been applied either with new sets of records #3 and #4 or with the sets of records used for IDA, but scaled to the new target acceleration, for both *IM*. This approach was used in order to investigate the influence of records selection on the decision making based on 3R methods. MSA involved totally different sets of *GMs*. Since ground motions varies with respect to the intensity, many different sets were selected (i.e. sets #5-19 in the case of *PGA*, #20-34 in the case of $S_a(0.28)$). Returning period of sets from #3 to #34 are various because *GMs* have been selected starting from a target value of acceleration, hence returning period must be directly read from the concerning hazard curve.

Table 1. Adopted sets of records.

Type of analysis	Target acceleration	No. of records in a set	Set
IDA	*PGA*	30	#1
	$S_a(0.28)$	30	#2
3R method (SSA)	*PGA*	30	#3
	$S_a(0.28)$	30	#4
MSA	*PGA*	30	#5-19
	$S_a(0.28)$	30	#20-34

5.2 Seismic Analysis

The investigated infrastructure was analyzed by IDA, MSA and SSA using ground motions selected according to Section 5.1. Results of IDA and MSA is *IM-EDP* relationship, which was used for the estimation of *IM* which causes exceedance of *LS* for a specific *GM*. The result of seismic analysis is thus a sample of intensities causing exceedance of limit state (IM_i in Equation 2 or 3), which was defined for the steel support structure and pipes according to the following *EDPs*:

- steel support structure strain;
- stress of the pipeline, which can be a rough indicator of operational limit state of pipe.

5.2.1 Definition of Limit State

Definition of *LS* is not an easy task because analyst should account for the constraints from the modelling, but on the other hand, the most important failure modes that may occur should be captured. In this respect, more accurate investigations are needed either for pipes and frame as studied by (Lignos & Krawinkler, 2011). However, in this preliminary study and concerning pipes, yielding stress has been considered as an indicator for potential issues with industrial operations, thinking about this value as the ultimate stress before cracks initialization. Actually, many authors during testing campaigns and researches found the lacks of adequacy of Codes in the definition of *LSs* or providing over conservative values as discussed by (Touboul et al., 2006). However, this will be investigated in further studies. The *LS* of the support structure was instead related to *NC* limit state. However, there are several different possibilities for definition of structural *LS*. For example, EN1998-3 (CEN, 2005) provides three different definitions of *LSs* as shown in Table 2.

Table 2. LSs definition according to EN1998-3.

Class of cross section	Limit State		
	DL	***SD***	***NC***
1	1.0 θy	6.0 θy	8.0 θy
2	0.25 θy	2.0 θy	3.0 θy

Code definition of *LS* in Table 2 is simplistic but also not convenient if structural elements are modeled

with elements with distributed plasticity (e.g. forceBeamColumn element of OpenSees). In order to solve this issue, it was decided to define the *LS* on the basis of fiber strains. A short parametric study was performed in order to obtain the limiting value of strain for near collapse *LS*. Following procedure was applied. Firstly, simple pushover analyses of a cantilever with various steel profiles and length were performed. Then for each element the rotation corresponding to yield of the first fiber of element was obtained. Finally, the *NC* strain was defined by sampling the strain which corresponded to a *NC* rotation, which was defined equal to eight times the yielding rotation. The results of parametric study showed that the strain which corresponds to *NC* rotation is practically not affected by steel profiles, length and boundary conditions. The obtained *NC* strain (0.028) has been assumed as *LS*, whose corresponding *EDP* is thus the ratio between strain and *LS*.

5.2.2 IDA Results

IDA curves are presented in Figure 2 and 3 for frame and pipes with S_a(0.28) and *PGA* as *IM*. Fragility parameters have been estimated by taking logarithms of each ground motion's *IM* value associated with onset of collapse, and computing their mean and standard deviation according to Equation 2. The maximum strain ratio and maximum stress ratio normalized to the corresponding value associated with *LS* is used, respectively as *EDP* for the steel support structure and the pipes. Large dispersion has been observed for IDA curves based on the maximum strain ratio (Figure 2a and 3a), even for low level of *IM*. Such a response is not surprising since supporting structure has no rigid diaphragms at the joints of equal elevation. However, the dispersion corresponding to *PGA* or S_a(0.28) causing *NC* limit state in the supporting structure is more or less equal, while the dispersion of *LS* S_a(0.28) for pipes is significantly lower than the corresponding value for *PGA*. The shape of the IDA curves based on the maximum stress ratio is different. In fact, these IDA curves have the opposite curvature with respect to IDA curves corresponding to the supporting structure, since the increment of stress occurred in pipes is very small after the yield stress (strain). S_a(0.28) is probably the best *IM* for pipes since the dispersion for *LS* intensity for pipes is lower in the case of S_a(0.28). It is emphasized that the stress in the pipes was smaller than the yield stress for some *GMs*, because the *NC* limit state in the supporting structure occurred prior yielding of pipes.

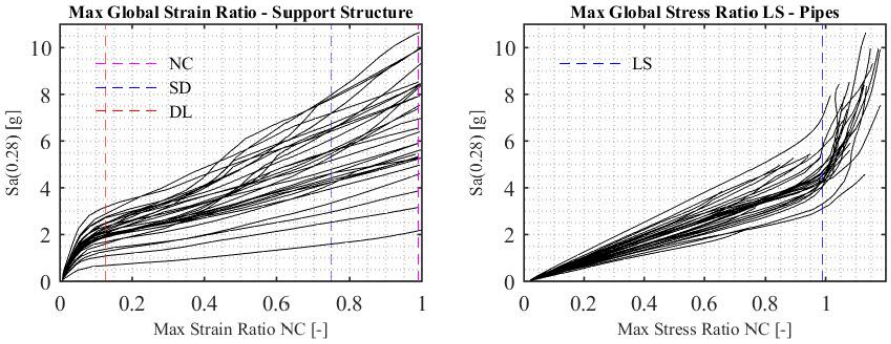

Figure 2. IDA Curves for the (a) steel support structure and (b) pipes based on S_a(0.28).

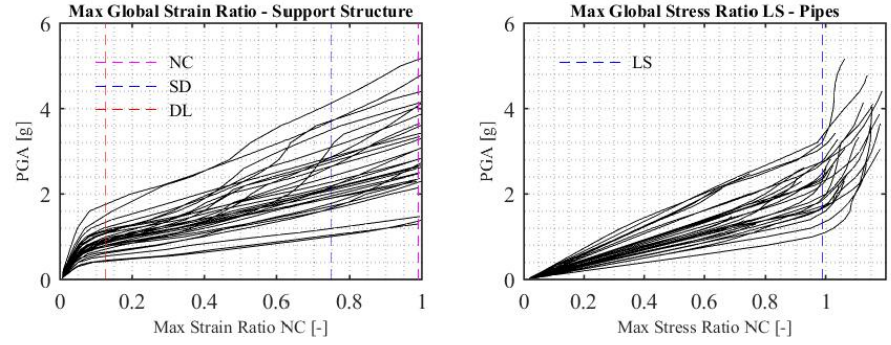

Figure 3. IDA Curves for (a) the steel support structure and (b) pipes based on *PGA*.

5.2.3 MSA Results

Figure 4 and 6 present results for frame and pipes respectively. Each dot represent the maximum *EDP* observed in one nonlinear dynamic analysis for a given *GM*. The dispersion of *EDPs* given a certain level of *IM* is quite large. However, one particular ground motion caused very large *EDP* with respect to the others (e.g. Figure 4a). This is a consequence of very adverse frequency content of that ground motion, which is highlighted in Figure 5. Moreover, the effect of plasticity can also be observed in Figure 4 and 6. The large dispersion is observed even for low levels of intensity.

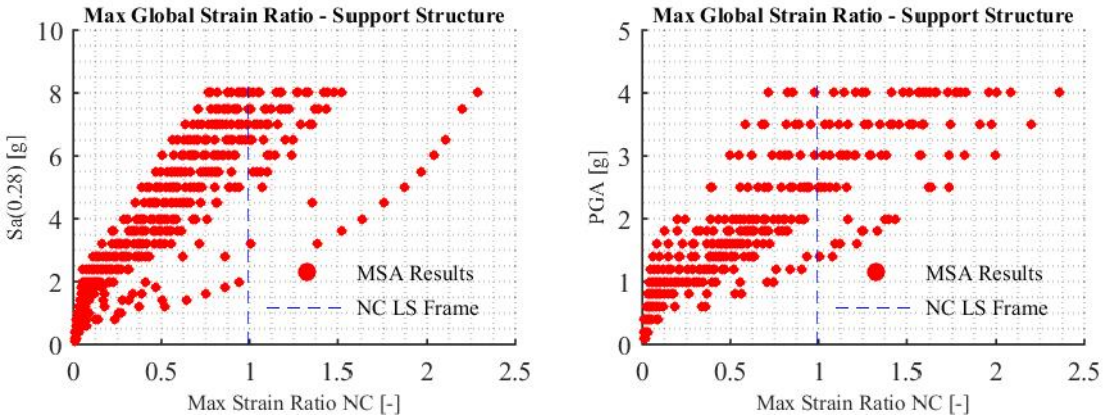

Figure 4. MSA for the steel support structure. Left (a) *IM* S_a(0.28), right (b) *IM PGA*.

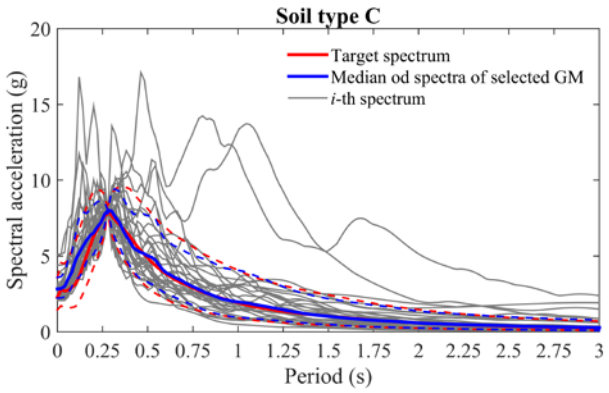

Figure 5. MSA set of ground motions #34.

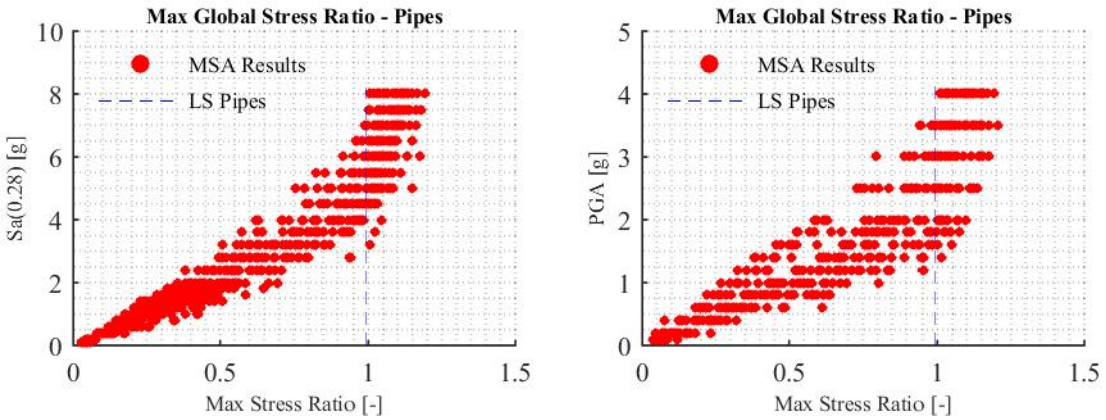

Figure 6. MSA for pipes. Left (a) *IM* S_a(0.28), right (b) *IM PGA*.

6. FRAGILITY ANALYSIS

The samples of values of intensity measures which cause exceedance of limit state were used to calculate θ and β (Table 3) according to Equation 2 and 3, respectively, for IDA and MSA. Resulting fragility curves are presented in Figure 7 and 8, respectively, for pipes and steel support structure. In order to get some feeling about the median value of intensity measure causing limit state (θ), the ratio between θ and the design value of intensity measure corresponding to return period of 2475 years (θ_{2475}) is presented in Table 4. It can be clearly observed that these ratios are not constant and that they are significantly larger than 1, which is a necessary condition in order to guaranty and adequate reliability.

Table 3. Dispersion and median.

		IDA		**MSA**	
		β	θ **[g]**	β	θ **[g]**
PGA	Pipes	0.30	2.13	0.29	2.38
	Frame	0.32	3.01	0.37	2.76
S_a(0.28)	Pipes	0.17	4.53	0.18	4.90
	Frame	0.37	6.62	0.39	7.87

Table 4. Ratio between median *IM* and code acceleration.

		IDA	**MSA**
		θ/θ_{2475}	θ/θ_{2475}
PGA	Pipes	3.28	3.66
	Frame	4.63	4.25
S_a(0.28)	Pipes	2.80	3.02
	Frame	4.09	4.86

The vulnerability of pipes is greater than the vulnerability of supporting structure for the *NC* limit state. It is quite interesting that the vulnerability of both components is quite similar if limit state of *SD* is the target limit state for the structure. This is much more evident in Figure 7b where fragility curves for pipes and *SD* limit state of the structure are almost the same. In Figure 8a it can be observed that the fraction of collapse obtained by MSA for a seismic intensity level in the interval from 4g to 6 g is almost constant. This outcome can be attributed to large sensitivity of MSA at the levels of intensities corresponding to low percentiles of fragility function. This sensitivity can be partly eliminated by increasing the number of ground motions for this levels of intensities.

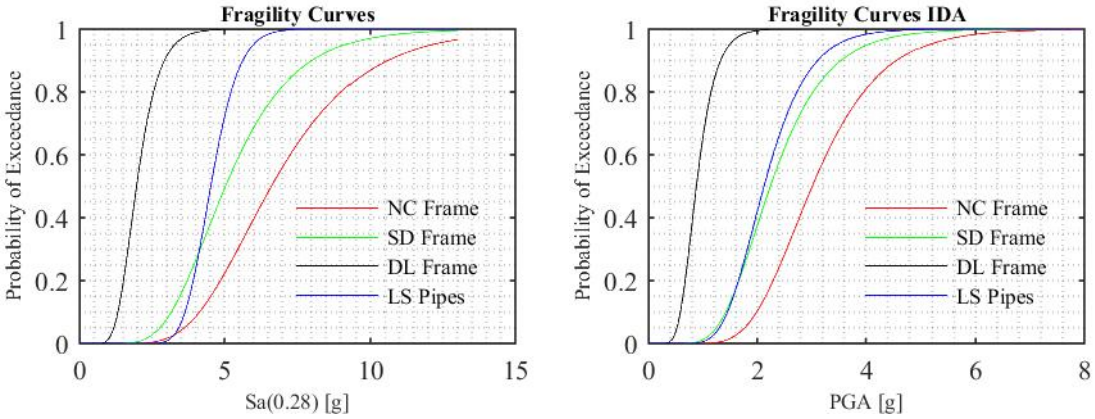

Figure 7. Fragility curves frame and pipes - IDA. Left (a) *IM* S_a(0.28), right (b) *IM PGA*.

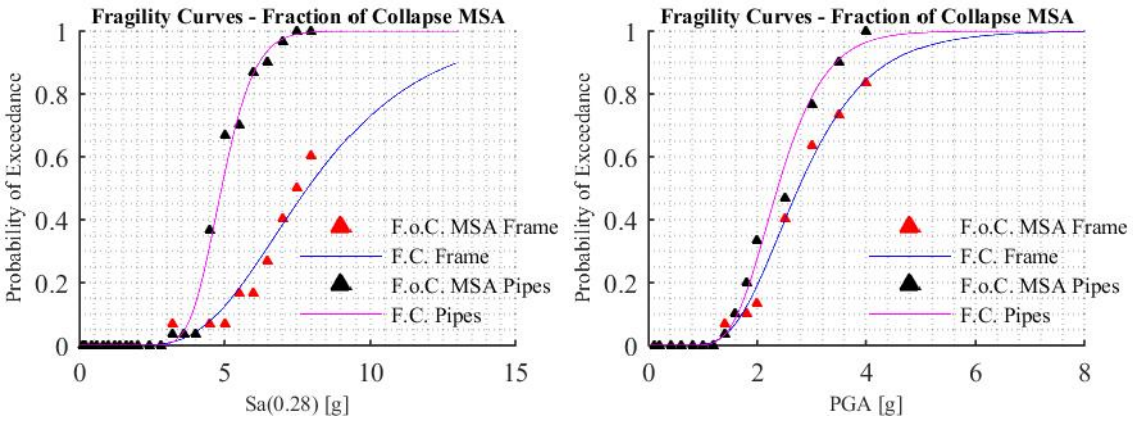

Figure 8. Fragility curves for frame and pipes - MSA. Left (a) *IM* S_a(0.28), right (b) *IM PGA*.

7. 3R METHOD

The 3R method (Dolšek & Brozovič, 2016) was used in order to check if the fragility curves of the investigated structure are on the left or the right hand side of the target fragility curves, which can be obtained from target risk by assuming the shape of the fragility function and the standard deviation of natural logarithms of seismic intensity causing exceedance of limit state. The method can be applied in conjunction with pushover analysis or directly by a SSA. The later approach was used in this study. The risk-based decision making using 3R method is robust since it was found that the rotating the fragility function around low percentile value does not cause significant impact on risk estimation. Interested reader can refer to the theoretical background of the method (Dolšek & Brozovič, 2016). Basic steps of 3R method are as follows:

- definition of target collapse risk;
- obtain detailed information regarding seismic hazard;
- selection of characteristic percentile (e.g. 16th percentile), calculate target fragility function and the characteristic value of target collapse intensity S_{at};
- selection of ground motions corresponding to S_{at};
- perform non-linear time history analyses (i.e. single stripe analysis) in order to obtain the limit-state ratio, i.e. the percentile of ground motions causing exceedance of limit state.
- risk-based decision making on the basis of limit-state ratio.

The objective of this study was also to check the accuracy of risk-based decision making if the structure is analyzed by the 3R method. For this purpose, the 3R method was performed.

7.1 Characteristic value of target limit-state intensity

The characteristic value of target limit-state intensity $S_{a,ct}$ was calculated with consideration of the hazard curve at the site of the investigated structure. It was also necessary to assume the standard deviation of limit-state intensity in log domain. However, the error produced by this assumption is often very low. In fact, assuming different deviation, within a reasonable range of values (0.3-0.5), and analyzing the risk by means of the closed form solution, which is derived from the risk equation, it was shown that risk is not significantly affected by the choice of β (Dolšek & Brozovič, 2016). Therefore, β was equal to 0.4 for both *IMs*. The assumed value is also close to the results presented in Table 3, where standard deviation of limit-state intensity was evaluated based on IDA and MSA. However, the evaluated β for S_a(0.28) which caused exceedance of limit states in pipes was observed significantly lower than 0.4. In order to calculate $S_{a,ct}$, the median value of target limit-state intensity has been calculated according to close-form solution of risk equation (Dolšek & Brozovič, 2016) :

$$\tilde{S}_{a,t} = \left(\frac{k_0}{\lambda_t}\right)^{\frac{1}{k}} e^{0,5\,k\,\beta_t} \tag{4}$$

where k and k_0 represent, respectively, the slope and the intercept of the linear approximation of the hazard curve in log domain, λ_t is the target risk and β the standard deviation. The $S_{a,ct}$, which corresponds to the 16th percentile of target fragility function, was obtained by Equation 5:

$$S_{a,ct} = \tilde{S}_{a,t} e^{-\beta_t} \tag{5}$$

$S_{a,ct}$ was then used to select sets of records #3 and #4 based on *CS*. The values of $S_{a,ct}$ can be observed from Figure 9.

7.2 Single Stripe Analyses (SSA)

Results of SSA, which was performed at $S_{a,ct}$ associated with the target risk 1e-5, are presented in Figure 9 for supporting structure and pipes. The results can be used within the decision model of 3R method. The analyst has to evaluate so-called limit-state ratio, i.e. the ratio between the records that caused the exceedance of *LS* and the number of all records in a set (30). If the limit-state ratio is greater than the characteristic percentile (0.16), it can be decided that the estimated risk is greater than the target risk. There are several reasons that the characteristic value is selected at low percentile, i.e. 16th percentile as it was assumed in this paper. The most important reason was discussed in the previous section. An additional advantage is that the disaggregation of the seismic hazard, if needed for ground-motion selection, is not largely affected by uncertainties, while the *GM* scaling may not be necessary because current databases of strong ground motions offer more ground motions with recorded intensities close to the characteristic value of target intensity. Furthermore, it makes sense that the level of intensity for SSA belongs to the region of intensities with a large impact on the risk. It has been shown, as (Eads et al., 2013) that this level of intensity is always smaller than the median collapse intensity.

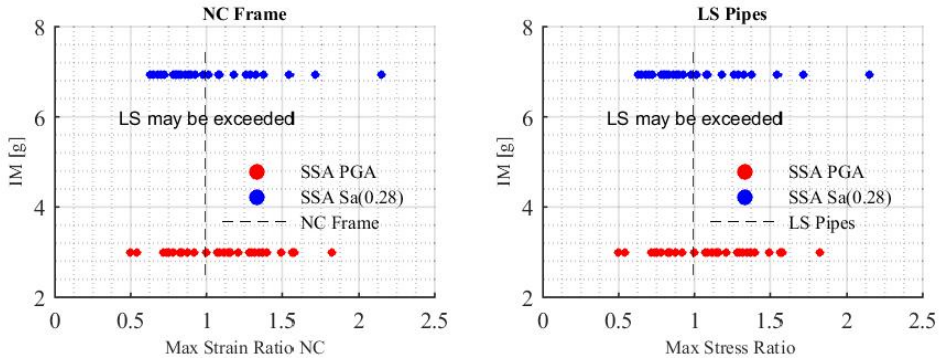

Figure 9. 3R results for (a) frame and (b) pipes with sets of records #3 and #4.

In order to make consistent comparison of the results and to better understand the influence of record selection, the SSA has been performed by using the ground motion set #1 and #2. The ground motion set #2 was used in IDA, but scaled to the characteristic value of target limit-state intensity. Results are presented in Table 5 where the limit-state ratio, i.e. the ratio between numbers of records that caused the *LS* exceedance and the number of all ground motions, is presented for support structure and pipes respectively. Note that the risk-based decision making was made for three levels of target risk (1e-5, 2e-5, 3e-5). From the results for the structure it can be observed that the risk for exceedance *NC* limit state in the supporting structure is greater than 2e-5 since limit-state ratio is greater than 16%. The only exception was the decision based on the ground motion set #4 and the target risk 2e-5. For this case, the limit-state ration was equal to 10%. It can also be observed that the risk for exceeding limit state of pipes is greater than 3e-5 since all limit-state ratios presented in Table 5 for pipes are greater than 16%. Based

on the parametric study it can be concluded, at least for the investigated facility, that the risk-based decision making is not significantly dependent on the selection of ground motions and the *IM*. However, in one case (target risk 2e-5, structure) the decision was observed inconsistent. In order to check which decision is correct, the risk was estimated and the results are discussed in next section.

Table 5. The limit-state ratio (in percent) for different target risk, different sets of records (IMs), supporting structure and piping system.

Target Risk			
1e-5	**2e-5**	**3e-5**	**Set of Records**
Structure - Pipes	**Structure - Pipes**	**Structure - Pipes**	
70% - 93%	40% - 70%	13% - 57%	#1 (IDA, *PGA*)
50% - 97%	17% - 67%	10% - 23%	#2 (IDA, $S_a(0.28)$)
60% - 87%	30% - 47%	13% - 27%	#3 (SSA, *PGA*)
40% - 93%	10% - 63%	13% - 37%	#4 (SSA, $S_a(0.28)$)

7.3 Discussion

The risk for limit state exceedance of the structure and the pipes was estimated using the fragility function based on IDA and MSA by taking into account both intensity measure and different sets of ground motions. The results are presented in Table 6 where it is also shown the decision from the 3R method. The results of 3R method are indicated by "*L*", which means that the outcome of the 3R method was that the risk is lower than the target risk, and by "*G*" that the risk is greater than the target risk. Firstly, it can be observed that the risk of exceeding limit state for pipes is around two times greater than the risk of exceeding near collapse limit state of the structure, which can be observed also by comparing estimated fragility functions (Figure 10). In addition, the risk of exceeding limit state for pipes is significantly greater than the selected target risks used in the 3R method. As a consequence, the risk-based decision making from the 3R method was always correct.

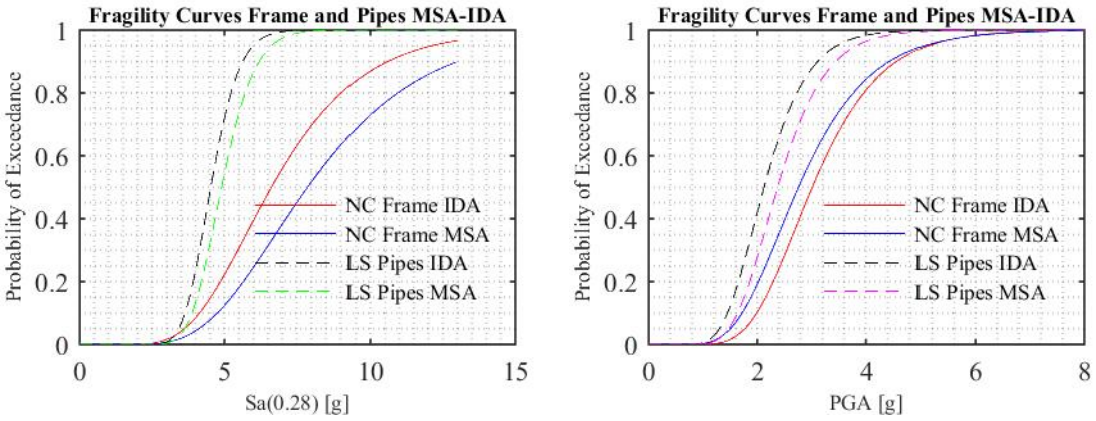

Figure 10. Frame fragility curves comparison. Left (a) *IM* $S_a(0.28)$, right (b) *IM PGA*.

The discussion on the results for the structure is not so straightforward. From the results it can be observed that the risk estimation is affected by the method and the *IM* used for the evaluation of the fragility function. Such an outcome could also be concluded by comparing fragility curves (Figure 10). It is very difficult to claim which result for risk are the most accurate. Since the dispersion of limit-state *PGA* for structure was slightly lower than the corresponding dispersion $S_a(0.28)$ (Table 3), it may be true that the *PGA* is better measure for this particular structure while for pipes would be the opposite. Comparing the results of risk estimation and the decision making from 3R method it can be concluded that the 3R method provided correct results even in the cases when the estimated risk was very close to the target risk. For example, estimated risk based on *PGA* and MSA was equal to 2.98e-5, while the limit-state ratio from 3R method, when expressed in percent was equal to 13% which is lower than 16% and thus risk is lower than the target risk 3e-5 (marked as "*L*" in Table 6). It is worth to emphasize that

in the case when $S_a(0.28)$ was used as the *IM*, the decisions obtained by the 3R method for a target risk 2e-5 were different with respect to the type of ground motions used in SSA (ground motion set #2 and #4). This can be understood as the 3R method provide inconsistent decision making, but if the risk-based decision from 3R method is compared to the risk estimation based on IDA or MSA it can be observed that decision-making by the 3R method was correct in both cases since the estimated risk (MSA: 1.94e-5, IDA: 2.69e-5) is once below the target risk (2e-5) and once above. This means the when the results of the 3R method are compared to the estimated risk, it can be quite important to be consistent with the use of ground motion set in 3R method and the method used for risk estimation.

Table 6. Risk values and decision.

Risk	***PGA***	***S_a*(0.28)**	***PGA***	***S_a*(0.28)**
	Frame		**Pipes**	
IDA	2.21e-5	2.69e-5	4.85e-5	4.96e-5
MSA	2.98e-5	1.94e-5	3.69e-5	4.25e-5
Target Risk	Set #3 / Set #1	Set #4 / Set #2	Set #3 / Set #1	Set #4 / Set #2
3e-5	*L/L*	*L/L*	*G/G*	*G/G*
2e-5	*G/G*	*L/G*	*G/G*	*G/G*
1e-5	*G/G*	*G/G*	*G/G*	*G/G*

8. CONCLUSION

For the investigated facility and defined limit states for the structure and the pipes it was found that the risk of exceedance of yield stress in pipes is greater than the risk of exceedance of the near collapse limit state of the structure. In petrochemical plants such an outcome may not be acceptable if the consequences of the exceedance of limit state for pipes are greater (e.g. pollution, explosion) or equal to the consequence of near collapse of structure. The results of this study revealed that the risk estimation significantly depends on the type of analysis used for the evaluation of fragility function and the type of intensity measure. However, it is very difficult to claim which approach provides more accurate results. Probably MSA is more accurate method of analysis since it accounts for the variation of the target spectrum for ground motions selection, but, on the other hand it requires much more effort to select many sets of ground motions. Since the investigated facility does not have rigid diaphragms it is not so clear which intensity measure is better to be used in fragility analysis. The result indicated that in the case of structure the dispersion of near-collapse intensity was even slightly smaller for *PGA* rather than for the $S_a(0.28)$, which is usually not the case. However, the $S_a(0.28)$ can be considered better intensity measure for fragility analysis of the pipes, although further investigations are needed to better understand how important are the periods of the pipes for the selection of the intensity measure for fragility analysis of pipes. The 3R method was found very robust for risk-based decision making even in the case when the estimated risk, either based on IDA or MSA, was very close to the target risk prescribed in a 3R method. In addition, the type of *IM* used for risk estimation did not affect the accuracy of the 3R method. However, it is quite important to be consistent with the use of ground motion set when comparing results of risk estimation by the risk-based decision obtained by 3R method. It can be concluded that 3R method is computationally efficient since it requires nonlinear dynamic analyses at only one level of *IM*. Further investigations are, however, needed in order to better understand limitations of the 3R method.

9. ACKNOWLEDGMENTS

The work presented herein was carried out with a financial grant from H2020 Marie Skłodowska-Curie Innovative Training Network, within the research project XP-RESILIENCE (G.A. 721816).

10. REFERENCES

Akkar, S., Sandikkaya, M. a., Şenyurt, M., Azari Sisi, A., Ay, B.O., Traversa, P., Douglas, J., Cotton, F., Luzi, L., Hernandez, B., Godey, S. 2014. Reference database for seismic ground-motion in Europe (RESORCE). Bulletin Of Earthquake Engineering 12, 1: 311–339.

Aparna, D., Vinay k., G. 1998. RESPONSE OF MULTIPLY SUPPORTED SECONDARY SYSTEMS TO EARTHQUAKES IN FREQUENCY DOMAIN APARNA. EARTHQUAKE ENGINEERING AND STRUCTURAL DYNAMICS 27: 187–201.

Azizpour, O., Hosseisni, M. 2009. A verification of ASCE Recommended Guidelines for seismic evaluation and design of combination structures in petrochemical facilities. J. Of Applied Sciences 21, December 2009.

Baker, J. 2010. Conditional Mean Spectrum: Tool for Ground-Motion Selection. Journal Of Structural Engineering 137, 3: 322–331.

Baker, J.W. 2014. Efficient analytical fragility function fitting using dynamic structural analysis. Earthquake Spectra In-Press.

Bursi O.S., Paolacci F, Shahin R., Alessandri S., Tondini N., (2016), Seismic Assessment of Petrochemical Piping Systems Using a Performance-Based Approach, Journal of Pressure Vessel and Technology, Vol. 138:3 - DOI: 10.1115/1.4032111

Caprinozzi, S., M. Ahmed, M., Paolacci, F., Bursi, O.S., La Salandra, V. 2017. Univariate Fragility Models for Seismic Vulnerability Assessment. V: Pressure Vessels and Piping Conference. Waikoloa, United States, 16-20 july: 1–10 pp.

EN .1998–3:2005. Eurocode 8: Design of structures for earthquake resistance - Part 3: Assessment and retrofitting of buildings. Brussels, European Committee for Standardisation.

Chiou, B., Darragh, R., Gregor, N., Silva, W. 2008. NGA project strong-motion database. Earthquake Spectra 24, 1: 23–44.

CSI. 2011. SAP2000. Berkeley, California, USA, Computers & Structures INC.:

Dolšek, M., Brozovič, M. 2016. Seismic response analysis using characteristic ground motion records for risk-based decision-making (3R method). Earthquake Engineering & Structural Dynamics 45, 3: 401–420.

Eads, L., Miranda, E., Krawinkler, H., Lignos, D.G. 2013. An efficient method for estimating the collapse risk of structures in seismic regions. Earthquake Engineering & Structural Dynamics 42, 1: 25–41.

Jalayer, F. 2003. Direct probabilistic seismic analysis: Implementing non-linear dynamic assessment. Doctoral dissertation. Stanford, Stanford University, Department of Civil and Environmental Engineering:

Jayaram, N., Lin, T., Baker, J.W. 2011. A computationally efficient ground-motion selection algorithm for matching a target response spectrum mean and variance. Earthquake Spectra 27, 3: 797–815.

Lignos, D.G., Krawinkler, H. 2011. Deterioration Modeling of Steel Components in Support of Collapse Prediction of Steel Moment Frames under Earthquake Loading. Journal Of Structural Engineering 137, 11: 1291–1302.

MathWorks. 2012. MATLAB the Language of Technical Computing. MathWorks:

McKenna, F., Fenves, G.L. 2010. Open System for Earthquake Engineering Simulation (OpenSees). Pacific Earthquake Engineering Research Center: http://opensees.berkeley.edu

F. Paolacci, Md. S. Reza, O. S. Bursi, (2011). Seismic analysis and component design of refinery Piping systems COMPDYN 2011 -III ECCOMAS Thematic Conference on Computational Methods in Structural Dynamics and Earthquake Engineering, Corfu, Greece, 26–28 May 2011

Paolacci, F., Giannini, R., De Angelis, M. 2013. Seismic response mitigation of chemical plant components by passive control techniques. Journal Of Loss Prevention In The Process Industries 26, 5: 924–935.

Šebenik, Ž., Dolšek, M. 2016. Strong ground motion database. Ljubljana, University of Ljubljana, Faculty of Civil and Geodetic Engineering, IKPIR:

Task Committee on Seismic Evaluation and Design of Petrochemical Facilities of ASCE. 2011. Guidelines for Seismic Evaluation and Design of Petrochemical Facilities. Second Edi. American Society of Civil Engineers:

Touboul, F., Blay, N., Sollogoub, P., Chapuliot, S. 2006. Enhanced seismic criteria for piping. Nuclear Engineering And Design 236, 1: 1–9.

Vamvatsikos, D., Cornell, C.A. 2002. Incremental dynamic analysis. Earthquake Engineering & Structural Dynamics 31, 3: 491–514.

Woessner, J., Laurentiu, D., Giardini, D., Crowley, H., Cotton, F., Grünthal, G., Valensise, G., Arvidsson, R., Basili, R., Demircioglu, M.B., Hiemer, S., Meletti, C., Musson, R.W., Rovida, A.N., Sesetyan, K., Stucchi, M. 2015. The 2013 European Seismic Hazard Model: key components and results. Bulletin Of Earthquake Engineering 13, 12: 3553–3596.

Zentner, I. 2017. A general framework for the estimation of analytical fragility functions based on multivariate probability distributions. Structural Safety 64: 54–61.